U.S. DEPARTMENT OF ENERGY | Office of Science

DOE/SC-ARM-TR-276

Comparison of X1 (OLD) and X3 (NEW) Aerosol Observing Systems at the North Slope of Alaska NOAA Observatory

E Andrews

December 2021

ARM

DISCLAIMER

DOE/SC-ARM-TR-276

Comparison of X1 (OLD) and X3 (NEW) Aerosol Observing Systems at the North Slope of Alaska NOAA Observatory

E Andrews, National Oceanic and Atmospheric Administration

December 2021

Work supported by the U.S. Department of Energy,
Office of Science, Office of Biological and Environmental Research

Acknowledgments

- Andy Clarke for spending six weeks at BRW in October 2020 in the midst of COVID travel concerns to install the NEW aerosol system.
- Derek Hageman for setting up the software to log OLD and NEW systems together and to provide the U.S. Department of Energy (DOE)/Atmospheric Radiation Measurement (ARM) user facility with the data they need.
- Bryan Thomas, Peter Detwiler, and Ross Bergener for day-to-day technical operation of the National Oceanic and Atmospheric Administration (NOAA) Barrow Observatory aerosol system.

Acronyms and Abbreviations

AGL	above ground level
AOS	Aerosol Observing System
ARM	Atmospheric Radiation Measurement
BFR	backscattering fraction
BRW	NOAA Barrow Observatory
CLAP	continuous light absorption photometer
CPC	condensation particle counter
DOE	U.S. Department of Energy
NOAA	National Oceanic and Atmospheric Administration
NSA	North Slope of Alaska
PMT	photomultiplier tube
Rsp	submicron scattering fraction
SAE	scattering Angström exponent
WCCAP	World Calibration Centre for Aerosol Physics

Contents

Figures

Tables

1.0 Introduction

This report describes a comparison of the overlapping X1 and X3 Aerosol Observing Systems (AOS) at the North Slope of Alaska (NSA) observatory. Due to structural issues with the original observatory building, the National Oceanic and Atmospheric Administration (NOAA) funded the design and construction of a new observatory building. Construction began in 2019 and was completed in 2020. The now decommissioned old NOAA Barrow Observatory (BRW) housed the AOS referred to as an NSA external site X1 from October 1997 through August 2021. A new observatory building next door housed the AOS referred to as an NSA external site X3 starting in October 2020. In this document we will refer to the original observatory system measurements as 'OLD' and the measurements in the new building as 'NEW'.

While the old and new building are located right next to each other (Figure 1), the inlet height and sample lines differ between the OLD and NEW system due to constraints in each building. While it was thought that these differences are unlikely to have a significant impact on the long-term time series, it is best practice to perform an evaluation to ensure measurement continuity. Overlapping measurements were acquired in the two buildings for a subset of the AOS suite instrumentation for the time period October 2020−August 2021.

Figure 1. Image of old (left) and new (right) NOAA BRW observatory buildings, September 2021. (Photo: E. Andrews)

In October 2020 an AOS was installed in the new observatory building. The NEW components of the system included a nephelometer, particle counter, and impactor box sent up from NOAA. The continuous light absorption photometer (CLAP) and aethalometer (AE33) from the old building were moved into the new building and became part of the NEW AOS. Following this move, the OLD AOS consisted of the original nephelometer, particle counter, and impactor box. For both the OLD and NEW AOSs, the impactor box switches between a PM10 and PM1 impactor every 30 min, thus enabling measurement of scattering at two different sizes.

In the next sections we describe the differences in the sampling inlets, the measurements that were compared, and known uncertainties in the measurements. The uncertainties are important because they determine whether the observations agree.

2.0 Methods

2.1 Inlet System Differences for the AOSs

Table 1 highlights some of the differences between the OLD and NEW inlet system at BRW. It is unlikely that the slightly different stack heights and the different rainhat configurations had a significant impact on aerosol sampling, but for completeness they are noted here. The OLD inlet design is likely to have resulted in some particle losses (particularly larger particles) during transit from the flow splitter at the base of the stack to the instrument rack inside the building, due to longer sample line, more bends, and longer horizontal runs.

Table 1. Summary of inlet system differences.

Components	OLD inlet	NEW inlet
Rainhat	shallow cone, above stack[1] 	cylindrical, encasing stack[1] 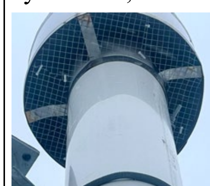  (angled view) (side view)
Insect screen	none	1/2” mesh
Stack height	~10 m AGL	~13 m AGL
Inlet line length from splitter at stack base	~4 m, with ~2.5 m horizontal run	~2 m, primarily angled, but with ~0.1 m horizontal run
Inlet line bends	three ~90° bends	one ~45° bend, one ~90° bend

[1] Pictures by Ross Burgener. Galvanized steel rainhat will be replaced in 2022 with stainless steel rainhat.

2.2 Parameters and Instruments for Comparison

Table 2 lists the instruments that were used for this comparison. The comparison does not include a measurement of aerosol absorption because a duplicate instrument was not available.

Table 2. Instruments used for comparison.

Instruments	Measurements	Old Building (X1)	New Building (X3)
Nephelometer, TSI model 3563	Total scattering coefficient (σ_{sp}) and back scattering coefficient (σ_{bsp}), at 450, 550, and 700 nm (unit: Mm^{-1})	s/n 1045	s/n 1083
Particle counter, TSI model 3010	Particle number concentration (unit: cm^{-3})	s/n 2452	s/n 2047

Several comparisons between the two systems can be done. First, the number concentrations from both buildings can be compared. Second, the scattering and backscattering coefficients can be compared. The scattering and backscattering coefficients can be compared for both the PM1 and PM10 size cut and for all three nephelometer wavelengths. Finally, some derived parameters − backscattering fraction (BFR), scattering Angström exponent (SAE), and sub-um scattering fraction (Rsp) − can be calculated and compared. Table 3 contains the equations for these three derived parameters.

Table 3. Equations for derived parameters compared in this study.

Derived Parameters	Equation
Backscattering fraction (BFR)	$BFR = \sigma_{bsp}/\sigma_{sp}$
Scattering Angström exponent (SAE)	[1]$SAE = -\log(\sigma_{sp,\lambda 1}/\sigma_{sp,\lambda 2})/\log(\lambda_1/\lambda_2)$
Submicron scattering fraction (Rsp)	[2]$Rsp = \sigma_{sp,PM1}/\sigma_{sp,PM10}$

2.3 Uncertainties

TSI's product datasheet suggests 10% is the accuracy for the 3010 condensation particle counter (CPC). We have used that as the uncertainty here. That said, we only deploy CPCs to sites that agree to within 5% with our reference counter, which has been calibrated at the World Calibration Centre for Aerosol Physics in Leipzig, German (https://wccap.wmo-gaw-wcc-aerosol-physics.org/index.html).

The supplemental materials of Sherman et al. (2015) provide calculated uncertainties for hourly averaged nephelometer measurements and derived parameters. These uncertainties were calculated based on loadings for continental sites in the U.S. and may be on the low end for measurements at Barrow, which tend to have lower loading. Table 4 lists the variables and their uncertainty estimates from Sherman et al. (2015). Table 4 only listed the uncertainty values for the 550-nm wavelength parameters (550/450-nm wavelength pair for scattering Angström exponent). There are slight differences as a function of wavelength, but these are generally representative of the uncertainties for each parameter.

Table 4. Uncertainties for nephelometer measurements and derived parameters, from Sherman et al. (2015).

Variable	$\sigma_{sp,PM10}$ ($\sigma_{sp,PM1}$)	$\sigma_{bsp,PM10}$ ($\sigma_{bsp,PM1}$)	BFR (PM10)	SAE (PM10)	Rsp
%Uncertainty	9.2 (8.0)	8.9 (8.1)	2.6	1.8	2.7

3.0 Results

In this section we present the plots showing the intercomparisons of the various parameters. We start with number concentration and the spectral scattering and backscattering coefficients as a function of size cut and then show results for the derived parameters. Finally, we considered the effects of windspeed and operations on the observations for the OLD and NEW inlet.

3.1 Number Concentration

Particle number concentrations from the two CPCs were compared over the period of measurement. The plot on the left in Figure 2 shows the relationship between the instrument in the new building and the instrument in the old building. The particle number concentrations are well correlated, but based on the slope (slope= 0.86) the instrument in the old building reported values that were about 15% lower than those from the instrument in the new building. The plot on the right in Figure 2 shows the diurnal cycle for the two instruments with the shading indicating a 10% range. The 10% ranges clearly overlap, suggesting the instruments agree to within the manufacturer's suggested accuracy although there is a clear bias, with the older measurements being lower.

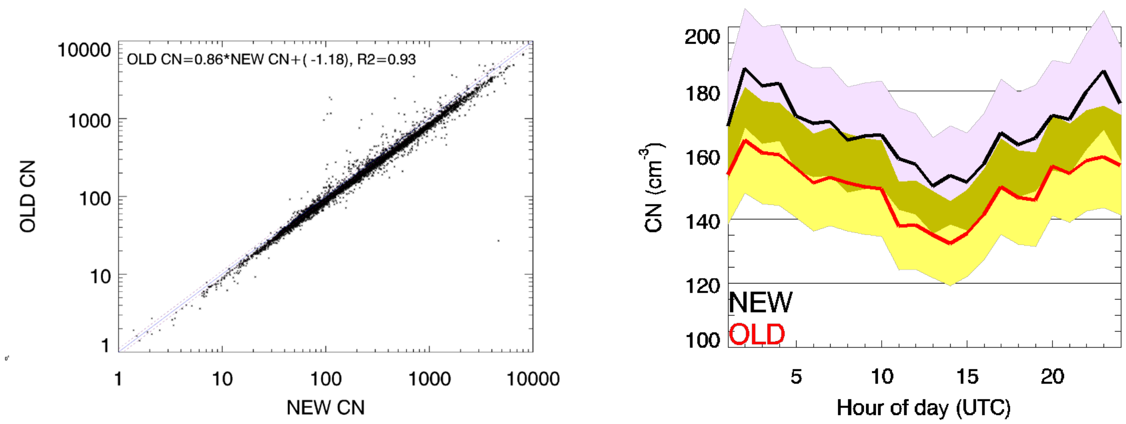

Figure 2. (left) Scatter plot of particle number concentration in the OLD and NEW systems. (right) Diurnal variability of number concentration – yellow and purple shading represents 10% spread of OLD and NEW systems, respectively; olive shading is overlap. Dashed purple lines in left figure indicate 10% uncertainty.

During the annual maintenance visit in late August, 2021, a short overnight side-by-side comparison with NOAA's transfer standard particle counter and the particle counter in the old building was done. The NOAA reference instrument is tied to a particle counter that was evaluated at the World Calibration Centre for Aerosol Physics (WCCAP; https://wccap.wmo-gaw-wcc-aerosol-physics.org) in Leipzig, Germany. The two instruments were highly correlated R^2=1, but the OLD counter was ~29% lower (Figure 13), again consistent with the observation that the OLD counter was counting low. Unfortunately, the CPC in the new building developed issues (low flow and low counts) the week before the annual maintenance and calibration visit. While cleaning improved the NEW CN measurements (higher counts and flow back to what was expected), the comparisons of the NEW CN with both the OLD CN and the reference CN counter were inconsistent and deemed untrustworthy. The NEW instrument was shipped back to Boulder, Colorado for cleaning shortly after the maintenance visit.

3.2 PM10 Scattering and Backscattering Plots

Figures 3 and 4 show the relationship between scattering and backscattering for the three nephelometer wavelengths (450, 550. and 700 nm) during the overlap time period. Figure 3 is for the PM10 size cut and Figure 4 for the PM1 size cut. Some overall observations:

1. In general, the comparison looks excellent. The uncertainty in the nephelometer scattering coefficient measurements is approximately 8-10%. The slopes are between 0.91 and 1.05 and often close to 1, suggesting very good agreement within the expected uncertainties.
2. Correlations are better for total scattering than backscattering coefficient. The backscattering coefficient is approximately 10% of scattering coefficient, so the lower correlation for backscattering coefficient is probably due in large part to lower loading and less sensitivity.
3. Correlations are better for the PM10 size cut than for the PM1 size cut, likely due to the fact that PM10 covers a wider measurement range of scattering than PM1.
4. Correlations are better for the 450- and 500-nm comparisons than for the 700-nm comparisons. This is primarily because the red photomultiplier tube (PMT) in the TSI nephelometer is noisier than the blue and green PMTs. Another contribution is that the measured scattering range also decreases as wavelength increases.

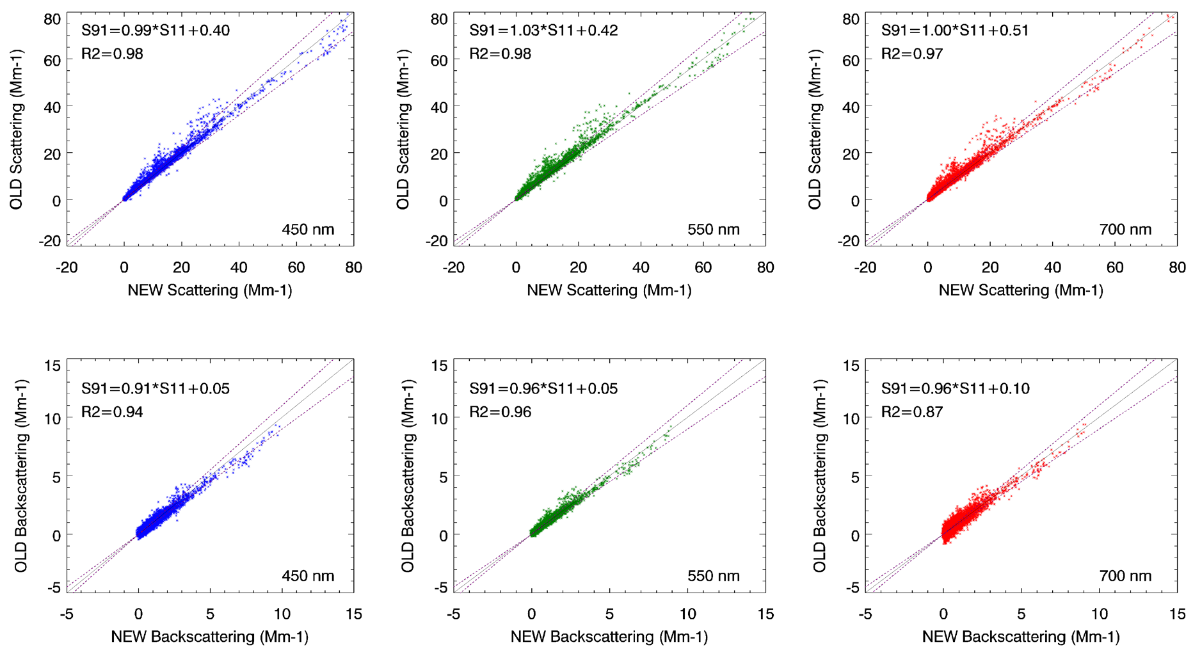

Figure 3. Scatter plots of relationship between OLD and NEW nephelometer for PM10 total scattering and backscattering coefficients for all three wavelengths. Dashed purple lines represent 10% uncertainty.

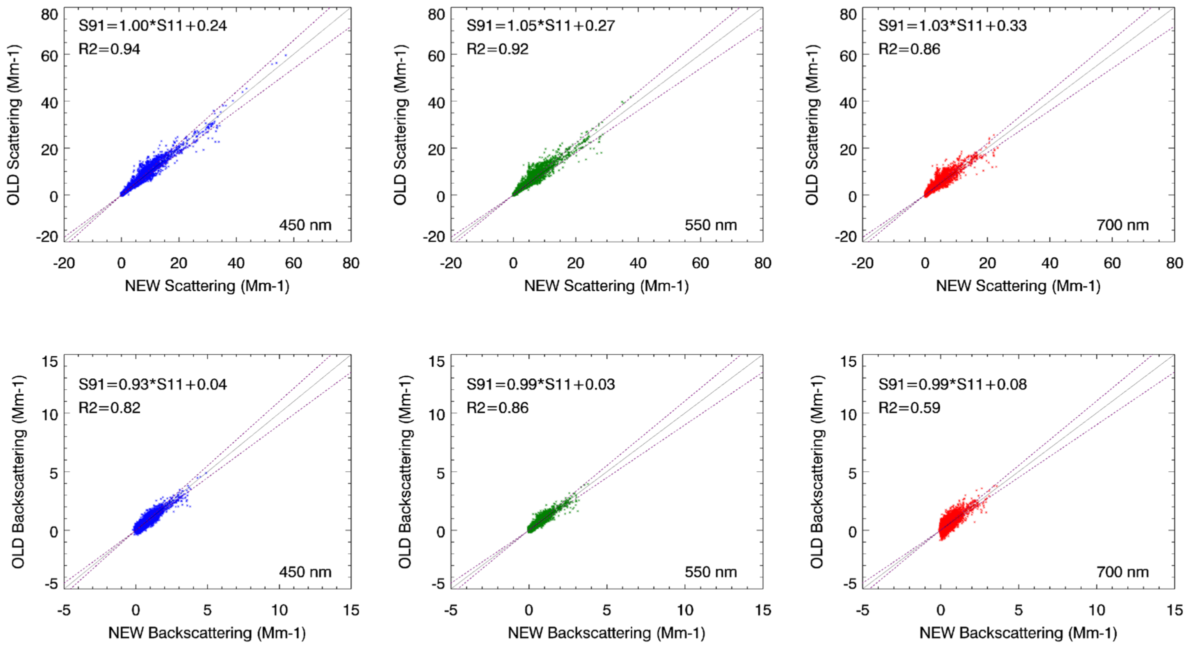

Figure 4. Scatter plots of relationship between OLD and NEW system nephelometer for PM1 total scattering and backscattering coefficients for all three wavelengths.

3.3 Derived Parameters

In addition to aerosol loading, which is represented by the spectral scattering and backscattering coefficients, we can also look at properties that are independent of loading. Figure 5 shows the relationship between PM10 backscattering fraction, scattering Angström exponent, and sub-micron scattering fraction for the nephelometers in the old and new building. To calculate these properties a constraint was applied requiring the PM10 550-nm scattering coefficient to be greater than 1 Mm^{-1}. This helps to eliminate noise in the calculated properties to low signal-to-noise ratios when aerosol loading is low (Delene and Ogren 2002).

For backscattering fraction, the top row of Figure 5 shows that there is really not a lot of variability in the range of BFR. The exception is for the 700-nm backscattering fraction derived from the nephelometer in the old building which exhibits a much wider range of values than observed for the nephelometer in the new building. Recall that the 700-nm backscattering coefficients exhibited the least correlation of the six plots presented in Figure 3. The correlation for BFR almost doubles when a scattering coefficient constraint of 5 or 10 Mm^{-1} is used, but is still quite low (R^2~0.5, see Table 5).

The middle row of plots in Figure 5 shows the scattering Angström exponent for various wavelength pairs. Scattering Angström exponents for all three wavelength pairs appear to be correlated, but the correlation is best for the wavelength pair that does not include the 700-nm measurements. Again, recall that the 700-nm scattering coefficients were the least correlated of the three nephelometer wavelengths. Even for the 450/550-nm pair, the R^2 value is only 0.65. If a scattering coefficient constraint of 5 or 10 Mm^{-1} is used, the correlation improves to R^2~0.9 (see Table 5), indicating that most of the noise is caused by taking the log of the ratio of two small numbers.

The last row of plots in Figure 5 shows the relationship between sub-micron scattering fraction for the OLD and NEW systems. The correlations are similar to those observed for scattering Angström exponent. The 450- and 550-nm wavelength comparisons are, again, better than the 700-nm wavelength comparison. There does appear to be a group of points (NEW system Rsp in the 0.5-0.7 range, OLD system Rsp in the 0.6-0.8 range) that may indicate sampling differences between the two systems. As alluded to above, such differences may be due to windspeed impacting sampling, and we will explore the effect of windspeed below. However, the fact that similar groupings do not occur in the SAE plots suggests that these clusters of points could be due to an issue with the impactor size cuts in one of the aerosol racks.

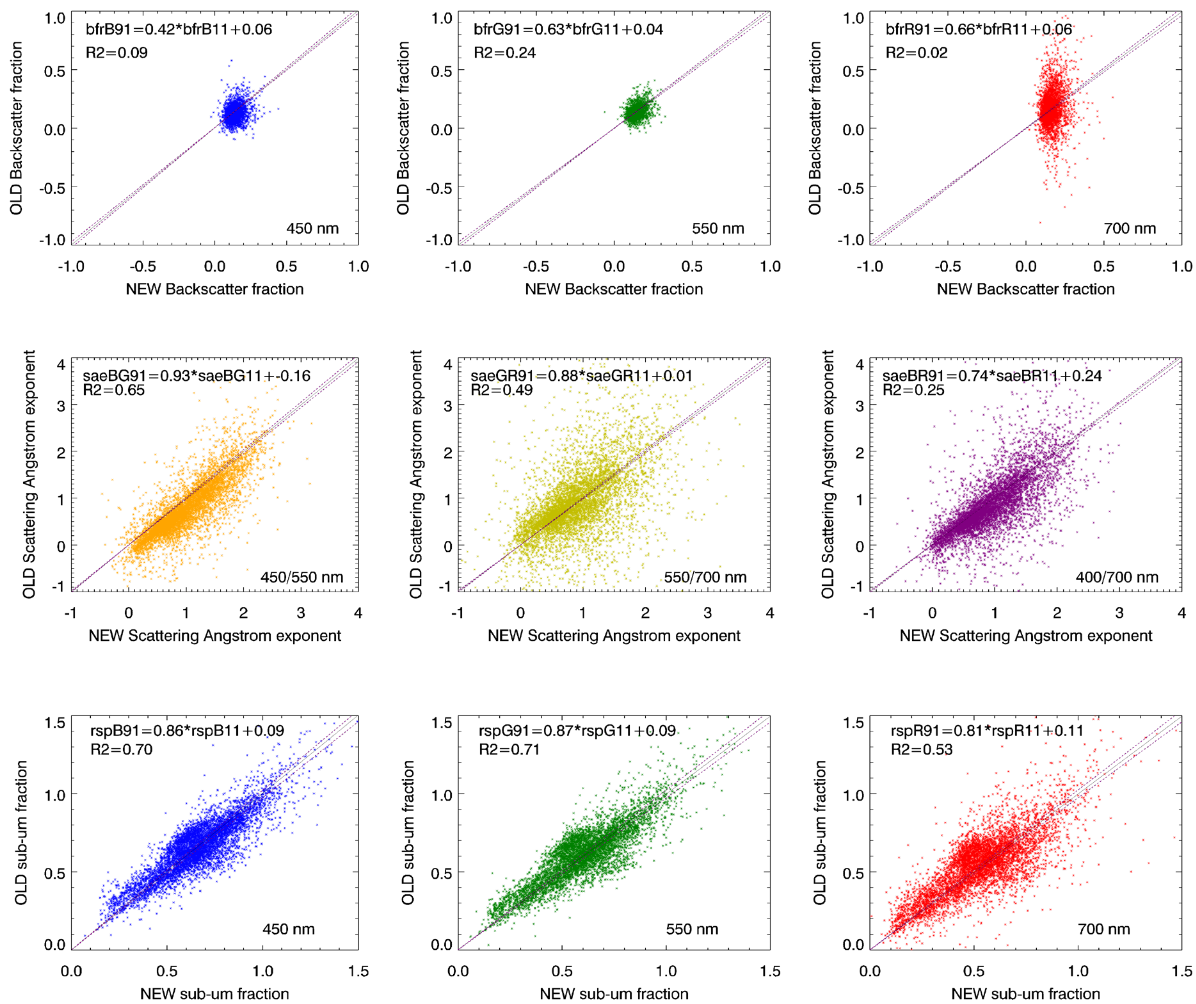

Figure 5. Relationships between derived parameters for OLD and NEW system. (top) Backscattering fraction (top); scattering Angström exponent(middle); Sub-micron fraction (bottom). Measurement wavelengths are indicated on the plots. Derived parameter values calculated for 550-nm PM10 scattering coefficient > 1 Mm^{-1}. Dashed purple lines indicate uncertainties reported for each parameter in Table 4.

Table 5. Effect of different scattering coefficient constraints (σ_{sp} [550 nm] >) on derived parameter relationships[1] and correlations. %data column indicates the approximate percentage of total available data available to calculate derived parameter after applying scattering coefficient constraint. (Percentage differs by slightly (±1%) depending on parameter.)

σ_{sp} (550 nm) >	BFR (550 nm)	SAE (450/550 nm)	Rsp (550 nm)	%Data
1 Mm^{-1}	y=0.63x+0.04, R^2=0.24	y=0.93*x-0.16, R^2=0.65	y=0.87*x+0.09, R^2=0.71	~83%
5 Mm^{-1}	y=0.76x+0.02, R^2=0.47	y=0.96*x-0.19, R^2=0.87	y=0.85*x+0.10, R^2=0.72	~48%
10 Mm^{-1}	y=0.76x+0.02, R^2=0.56	y=0.97*x-0.19, R^2=0.91	y=0.91*x+0.07, R^2=0.69	~22%

[1] In the equations, y represents the OLD system parameter and x represents the NEW system parameter.

3.4 Short Side-By-Side Comparisons During Final System Checks

During the annual maintenance visit (August 28−September 4) the aerosol rack in the old building underwent final checks and calibrations while the aerosol rack in the new building also underwent calibrations. These checks included overnight filtered air checks on both nephelometers to assess instrument noise as well as overnight comparisons of the nephelometers side by side in the new observatory.

Results of the filtered air checks on the nephelometers suggested both instruments measured close to zero (mean scattering coefficient <0.2 Mm^{-1}, standard deviation<0.7 Mm^{-1}) over the ~18h period measuring filtered air. This suggests there were no leaks in the nephelometers or other instrumental problems.

The instruments also were set up side by side in the new building. For this side-by-side test the nephelometers sampled in series, with the OLD nephelometer sampling the exhaust of the NEW nephelometer. The plot in Figure 6 shows the time series plot for the side-by-side comparison. The site was in a particularly clean phase so the range of observed aerosol scattering is low for both instruments. The peak towards the end of the time series (at ~DOY 343.7), was generated by having the instruments sample laboratory air while vacuuming near the air intake.

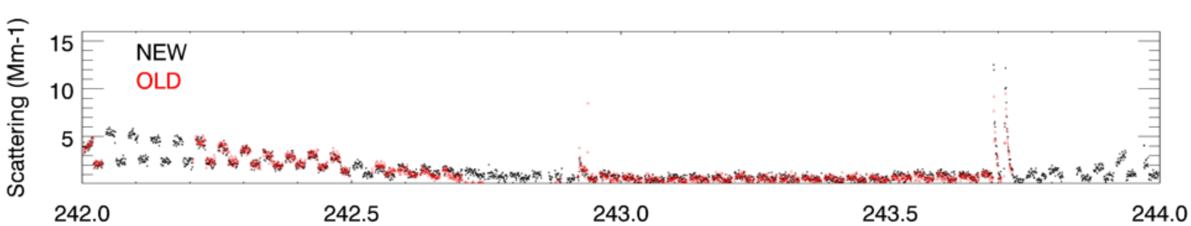

Figure 6. Time series plot of scattering coefficient (550nm) for 1-minute nephelometer data.

The time series shows that the two instruments track each other quite well. The segments of data on the time series plot occur when the impactor system switches between PM1 and PM10 size cut every 30 min. Figure 14 in the Appendix shows the xy scattering plot for the comparison. The correlation is R^2=0.83 and the slope for the linear regression is 1.00.

4.0 Discussion

Overall, there is quite good agreement between scattering coefficient and number concentration measurements for the two systems over the 11-month comparison period. The number concentration values from the OLD system are about 15% lower than the NEW system and the OLD counter is 29% lower than the reference counter, but the manufacturer suggested accuracy is ±10%. The OLD/NEW instruments agree to within that uncertainty (Figure 2), but there clearly is a slight bias with the OLD counter being lower.

The total scattering and backscattering coefficient comparisons are highly correlated and also within the reported instrument uncertainties, while the calculated parameters (BFR, SAE, Rsp) exhibit less correlation, due at least in part to all three quantities involving the ratios of small numbers. The calculated values are also often outside the uncertainty bounds listed in Table 4. As noted above, the uncertainties in Sherman et al. (2015) were calculated for sites with higher aerosol loads. Figures 15-16 in the Appendix show that if the derived properties are only calculated for higher levels of scattering (e.g., σ_{sp} [550 nm]>5 Mm^{-1}), the parameters are generally within the uncertainty bounds.

While measurement uncertainties related to the instruments lead to spread in the observations, inlet design and sampling differences can also cause discrepancies. Some external factors (e.g., windspeed and rainhat design) have been shown to impact aerosol sampling (e.g., Peterson et al. 2019 and references therein). To address this, we have looked at how the relationships change as a function of month of year as effects due to changes in atmospheric conditions may be more obvious in smaller time segments.

Figure 7 shows the relationship between the OLD and NEW system number concentration and PM10 scattering coefficient (for 550 nm) as a function of month of year. There are no clear temporal dependencies for number concentration. For the scattering coefficient, the two systems appear to be highly correlated for all months from April through December. However, there are a couple of groupings of points in the Jan/Feb/March plot that suggest some seasonal issues, with the OLD system reporting higher scattering than the NEW system. The question is whether these discrepancies are due to winds, inlet differences, or other system issues.

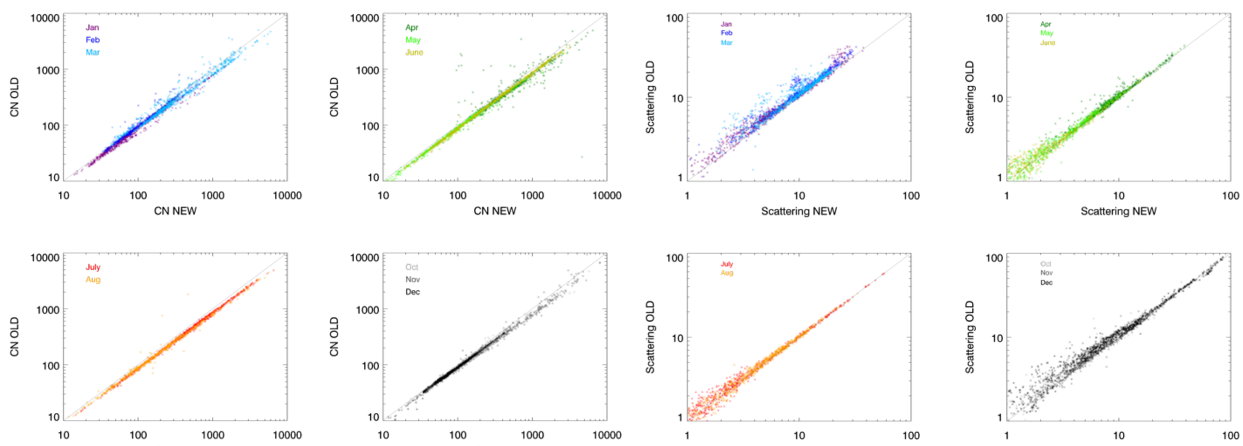

Figure 7. Monthly variation in particle number concentration and PM10 scattering coefficient (550 nm). Left four plots are CN; right four plots are scattering coefficient.

Unfortunately, the final windspeed data for the observatory are only available through May 2021. Wind data for June−August 2021 have not yet been reviewed by NOAA's observatory group. Conveniently, the available wind data encompasses January through March 2021, so we can consider whether windspeed is a cause for some of the discrepancies between the OLD and NEW AOS scattering variables in that time frame.

Figure 8 contains plot of parameters from the OLD and NEW system, colored as a function of windspeed. For the most part there do not appear to be clusters of points related to windspeed. The one exception is the group of points for 12 m s^{-1}<WS<14 m s^{-1} that suggests a possible wind effect on scattering and backscattering coefficient (OLD system has higher scattering than NEW system). Aside from those points, most of the data points in the 2 m s^{-1}<WS<14 m s^{-1} windspeed category lie on top of the data for the other windspeed categories − there is no clear windspeed effect.

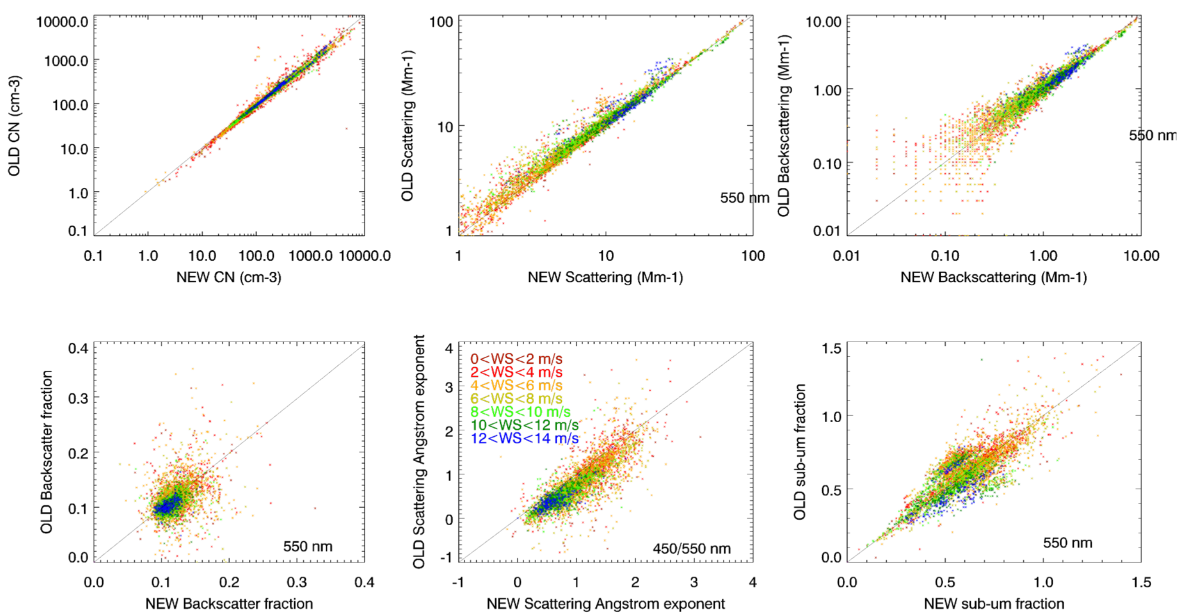

Figure 8. Relationship between selected OLD and NEW system parameters as a function of windspeed.

Figure 9 shows the systematic variability of parameters measured by the two systems as a function of windspeed. These plots also suggest that while there are differences between the two systems, the behavior as a function of windspeed is quite similar. An interesting side note from Figures 8 and 9 is that the highest windspeeds are associated with higher loading and larger particles (i.e., lower scattering Angström exponent), demonstrating the importance of wind-driven sea salt emissions at this remote site.

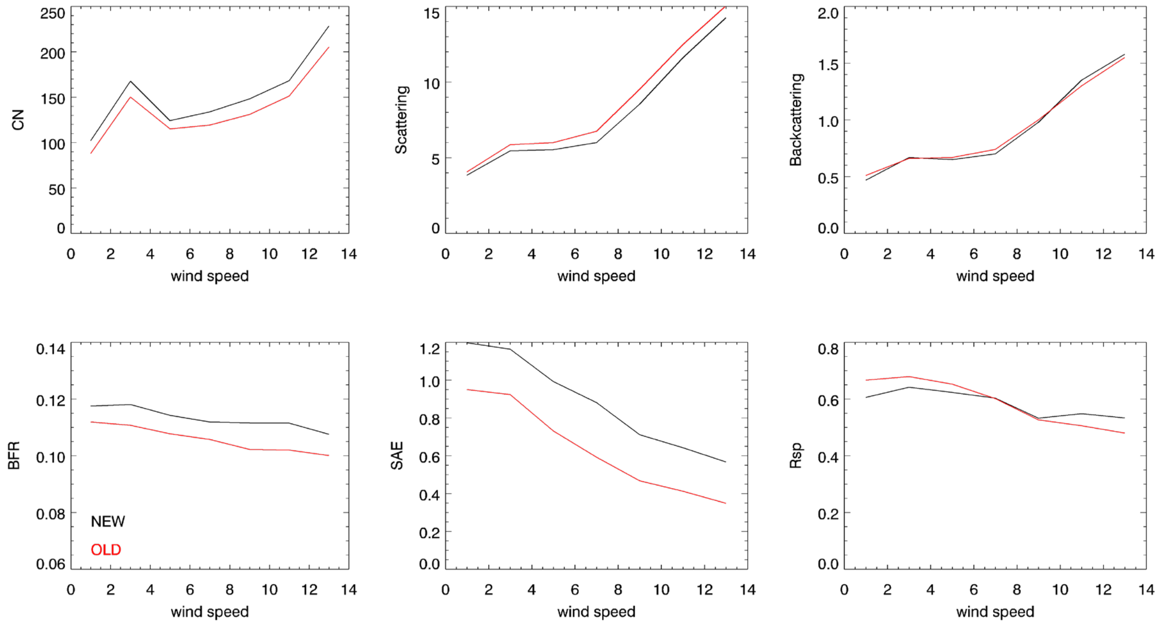

Figure 9. Systematic variability of OLD and NEW system parameters with windspeed.

So where does this leave us with respect to the seasonal differences in scattering coefficient that are seen in Figure 7? We have plotted the calculated parameters (BFR, SAE, and Rsp) as a function of month to see if we can gain any further insight. For the most part there appear to be no seasonal dependencies for these parameters (see Figures 17−19 in the Appendix). The one exception is for Rsp in January−March 2021 as shown in Figure 10, which shows distinct clusters for the three months.

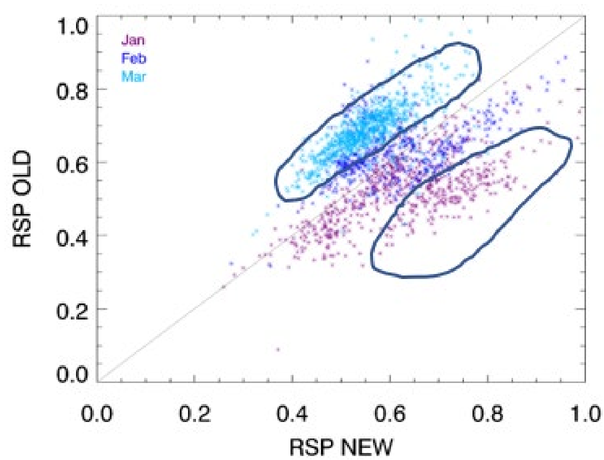

Figure 10. Sub-micron scattering fraction for OLD and NEW system for January, February, and March 2021. Circled areas indicate regions of particular concern.

When the windspeed is higher than 10 m s^{-1}, we tend to see that the NEW PM10 and PM1 scattering coefficients are lower than OLD PM10 PM1scattering coefficients, i.e., the ratio of NEW/OLD scattering dips below 1 (Figure 11). However, there are other times with low windspeed when that is also the case as well as times with high windspeed when the scattering for both systems does not appear to be affected.

The periods with low NEW/OLD scattering coefficient ratios exhibit no clear change in Rsp because both PM1 and PM10 NEW scattering coefficient are lower than PM1 and PM10 OLD scattering coefficient. These dips in the ratio of measured scattering coefficient suggest a potential issue with the NEW rain hat and/or sampling intake, but it is unclear how to further explore this with the information available. A quick analysis of the standard meteorology parameters measured at the site (e.g., pressure, temperature, dewpoint, relative humidity, windspeed and wind direction) when those data are available suggests that colder temperatures (ambient and dewpoint) and a more easterly wind may be connected with the periods when PM10 NEW scattering coefficient is lower than the PM10 OLD scattering coefficient, while ambient pressure, relative humidity, and windspeed are not. However, it is unclear what physical mechanism related to colder temperatures and easterly winds would affect inlet sampling efficiency. The changes in NEW/OLD scattering coefficient ratios do not appear to be related to the discrepancies in Rsp observed for the two systems; this is further discussed below.

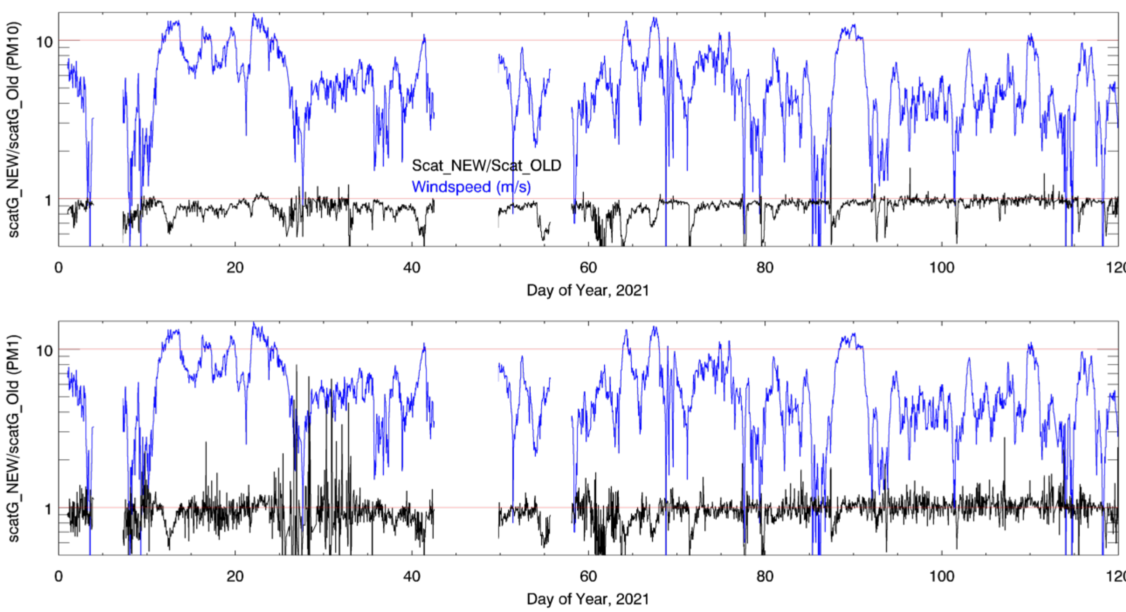

Figure 11. January−April 2021 time series of ratio of NEW to OLD scattering coefficient (black line) and windspeed (blue line). Top plot shows PM10 scattering ratio, bottom plot shows PM1 scattering ratio.

Figure 12 shows the time series of Rsp for the two systems. In two time periods, the Rsp values are different. The first occurs from January 15−23, 2021 and is the time period where Rsp from the OLD system is lower than the Rsp in the NEW system. The start date of this discrepancy corresponds to the size cut impactors being serviced in the NEW building while the impactors in the OLD building were not serviced. Rsp is the ratio of PM1/PM10 scattering coefficient (Table 3).

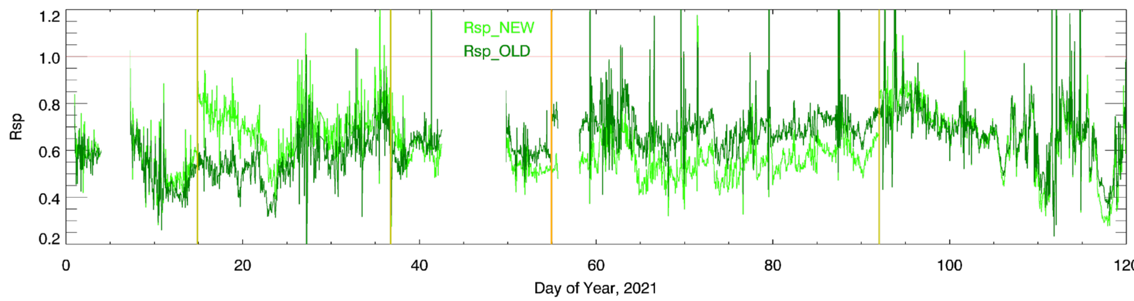

Figure 12. Time series of Rsp for OLD and NEW system for January through April, 2021. Mustard vertical lines (DOY 14.9, 36.75 and 92.9) indicate when NEW system impactors were cleaned, orange vertical line (DOY 54) indicates when OLD system impactors were cleaned.

The discrepancy for the January 15−23 time period is due to differences in the PM1 scattering coefficient − the PM1 scattering in the OLD building is lower than in the NEW building, likely due to buildup of particles in the impactor. The PM1 impactors have small holes that can readily clog and particles can also build up on the impaction plate. It is unclear what caused the end of the discrepancy in this case. January 23 was a Saturday and no activity was noted in the log (i.e.., impactor servicing) and nothing unusual appears in the housekeeping (no shifts in dP or T/P/RH/winds). Perhaps there was just enough new buildup in the impactors in the new building to make them consistent with the impactors in the OLD system that had not been serviced (since September 2020).

The other Rsp discrepancy occurs from mid-February to early April (February 23−April 2), with the OLD system Rsp being higher than the NEW system Rsp. This was the result of the OLD system impactors being cleaned on February 23 (DOY 54). This discrepancy ends when the NEW impactors are serviced on DOY 92 (April 2).

In both cases it appears that the impactor servicing (or lack thereof) caused the differences between the OLD and NEW system. It does not reflect a problem with the NEW aerosol system, but rather was the result of the technicians figuring out how to schedule impactor servicing for two aerosol racks. This highlights the importance of cleaning the impactors consistently and at least monthly at BRW.

5.0 Conclusions

In general, there is excellent agreement between the two systems. The OLD system CPC was approximately 15% lower than the NEW system CPC and 29% lower than NOAA's reference standard CPC, suggesting the OLD CPC could use an in-depth going over and 'tune up' in Boulder now that the OLD system has been shut down. The NEW CPC was sent back to Boulder for a thorough cleaning to deal with issues observed during the annual maintenance visit.

The nephelometer observations were within 10% (and usually much better) for all wavelengths and both size cuts for both total and backscattering coefficients. It is clear that the size cut impactors need to be serviced at least monthly at the site and that should be occurring going forward. There may be some differences between the OLD and NEW nephelometer measurements potentially related to system inlet design (rainhat), but those need more delving into and possibly some fluid mechanics analysis.

6.0 References

Delene, DJ, and JA Ogren. 2002. "Variability of aerosol optical properties at four North American surface monitoring sites." *Journal of the Atmospheric Sciences* 59(6): 1135−1150, https://doi.org/10.1175/1520-0469(2002)059<1135:VOAOPA>2.0.CO;2

Petersen, R, AG Hallar, IB McCubbin, JA Ogren, E Andrews, D Lowenthal, R Gorder, R Purcell, D Sleeth, and I Novosselov. 2019. "Numerical, wind-tunnel and atmospheric evaluation of a turbulent ground-based inlet sampling system." *Aerosol Science and Technology* 53(6): 712−727, https://doi.org/10.1080/02786826.2019.1602718

Sherman, JP, PJ Sheridan, JA Ogren, E Andrews, DC Hageman, L Schmeisser, A Jefferson, and A Sharma. 2015. "A multi-year study of lower tropospheric aerosol variability and systematic relationships from four North American regions." *Atmospheric Chemistry and Physics* 15(21): 12487−12517, https://doi.org/10.5194/acp-15-12487-2015

Appendix A

Supplemental Figures

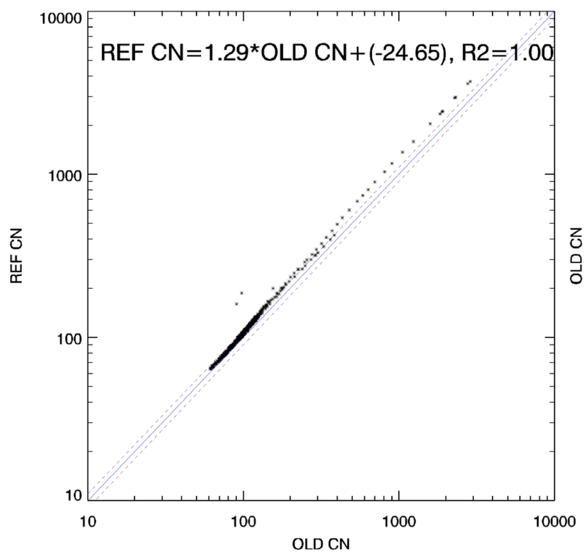

Figure 13. Scatter plot of overnight comparison test for OLD CN with NOAA reference counter.

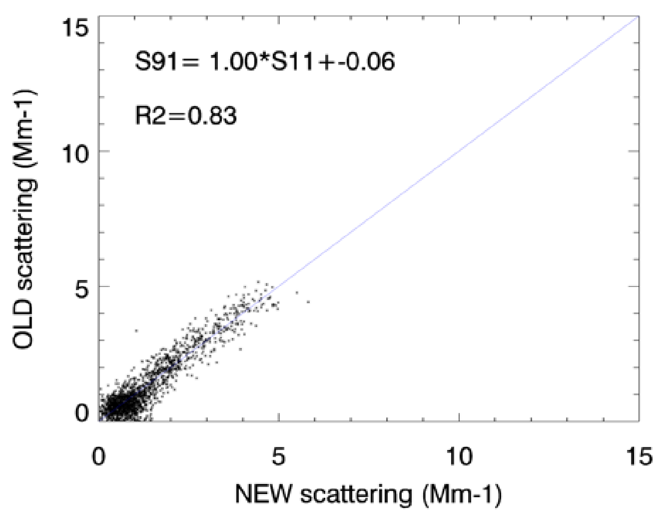

Figure 14. Scatter plots of overnight comparison test for 550-nm scattering coefficient with OLD and NEW nephelometers hooked up in series.

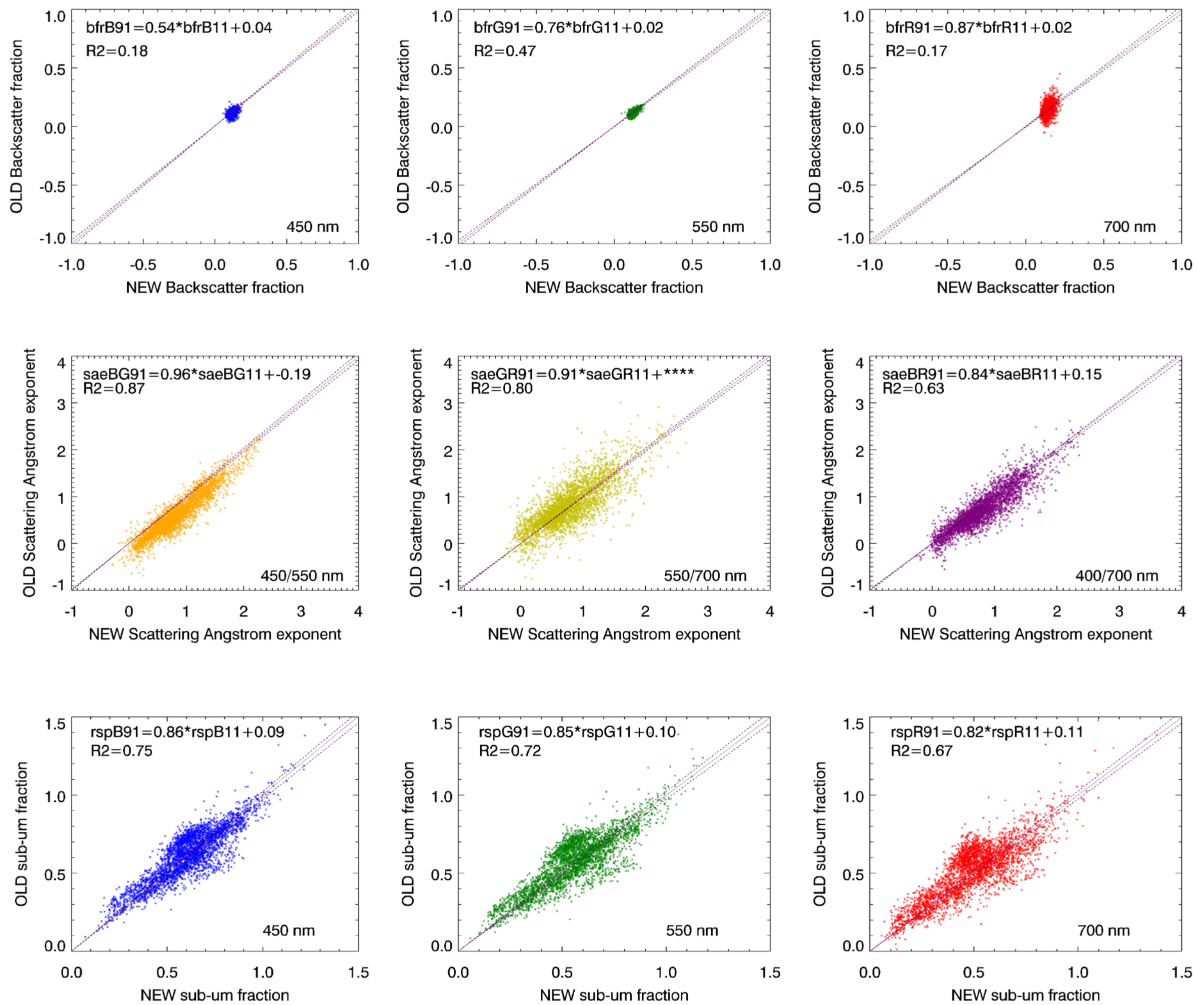

Figure 15. Derived parameters for scattering constraints (550-nm PM10 scattering coefficient > 5 Mm^{-1}). Dashed purple lines indicate measurement uncertainty (see Table 4).

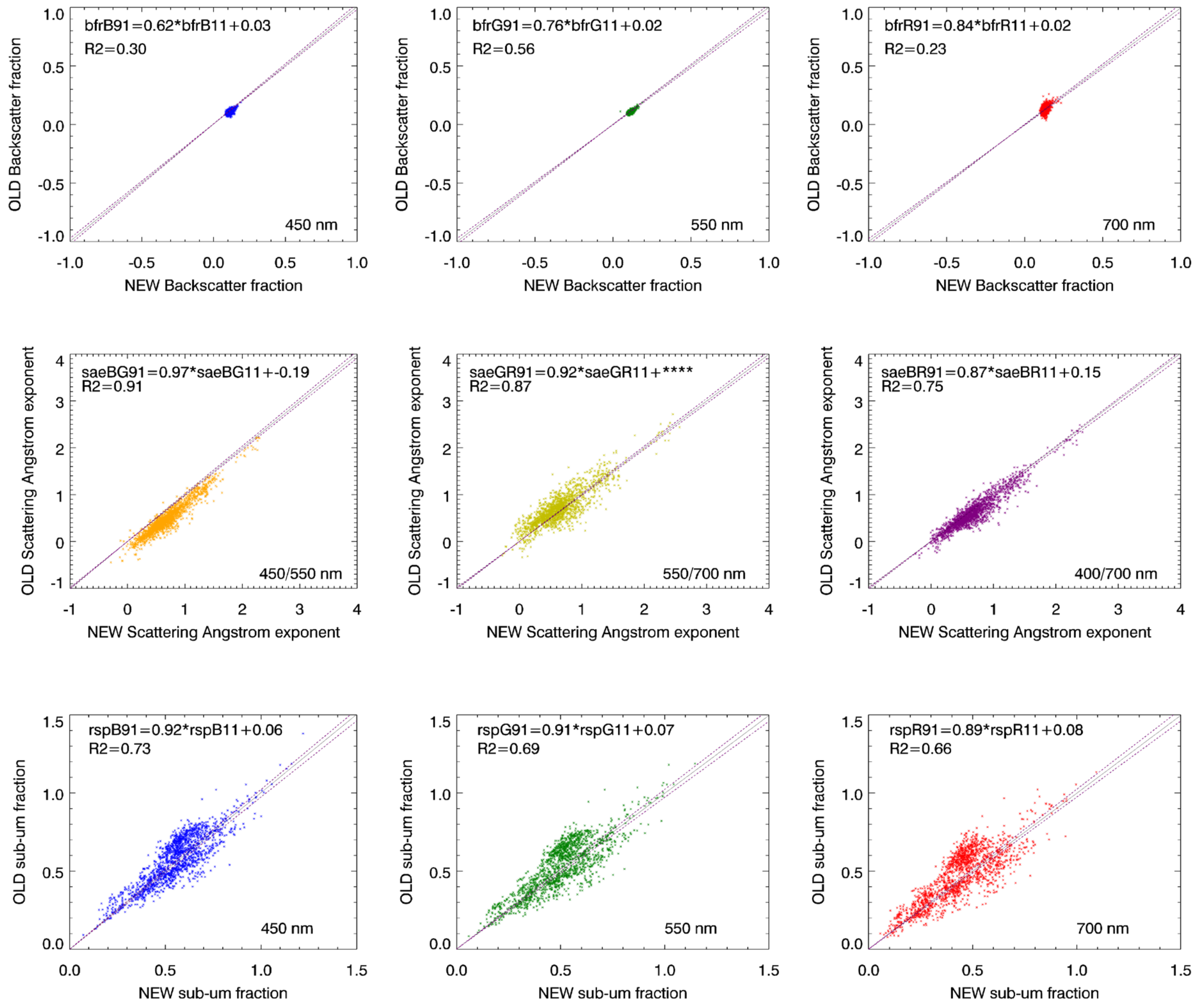

Figure 16. Derived parameters for scattering constraints (550-nm PM10 scattering coefficient > 10 Mm^{-1}). Dashed purple lines indicate measurement uncertainty (see Table 4).

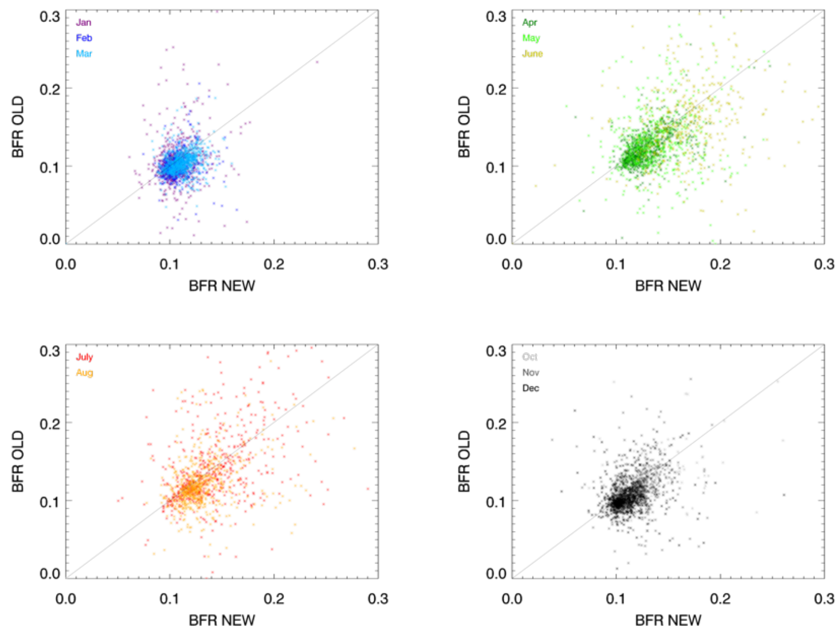

Figure 17. Monthly dependence of backscattering fraction.

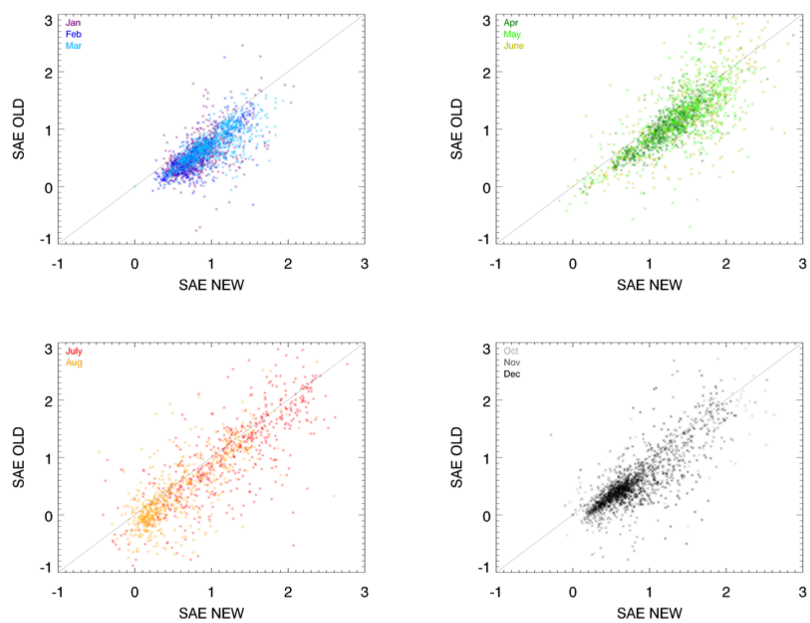

Figure 18. Monthly dependence of scattering Angström exponent.

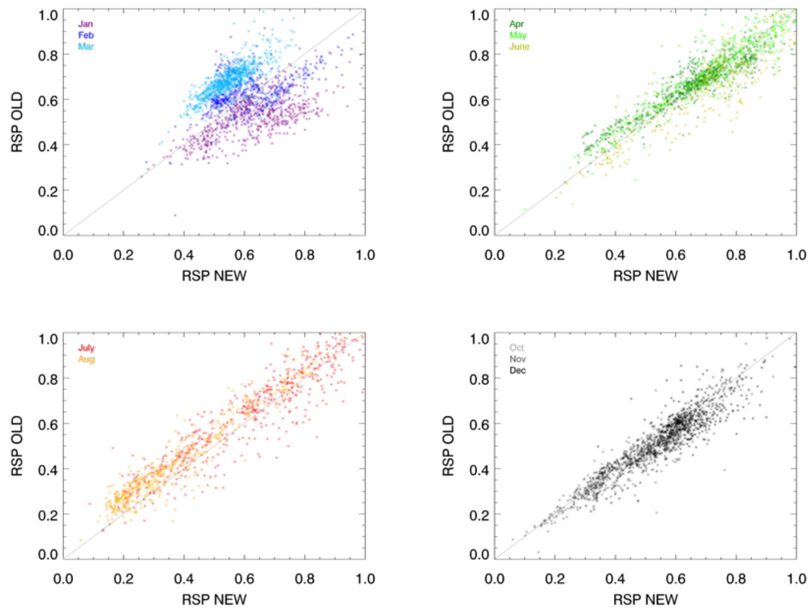

Figure 19. Monthly dependence of sub-micron scattering fraction.

ARM

www.arm.gov

U.S. DEPARTMENT OF ENERGY

Office of Science